Geogr. Fis. Dinam. Quat.
33 (2010), 45-60, 15 figg., 3 tabb.

ROBERTO RANZI (*), GIOVANNA GROSSI (*), ALESSANDRO GITTI (*) & STEFAN TASCHNER (*)

ENERGY AND MASS BALANCE OF THE MANDRONE GLACIER (ADAMELLO, CENTRAL ALPS)

ABSTRACT: RANZI R., GROSSI G., GITTI A. & TASCHNER S., *Energy and mass balance of the Mandrone glacier (Adamello, Central Alps).* (IT ISSN 0391-9838, 2010).

The Adamello Glacier is the largest glacierised area in the Italian Alps and consists of five hydrographic units, the major in size being the Mandrone Glacier which covered an area of 13.38 km^2 in June 2003.

In order to assess the yearly mass balance of the Mandrone Glacier the PDSLIM energy-balance model was applied: it is a seasonal snowpack model, adapted to glaciers and based on a distributed physically-based two-layer snow and ice scheme. In this paper the investigated area, the model and the hydrometeorological data used in input to the model and for its verification are described. On a large scale, the accuracy of the model in simulating the retreat of the snow covered areas during the melt season is verified through comparison with remote images, resulting in a 86% correspondence of observed snow-covered pixels. Downstream runoff measurements at the outlet of the Sarca di Genova basin at the Ponte Maria station were used as a term of comparison of the simulated summer melt. Runoff volumes measured over a twelve year period (1995-2006) were used to validate the simulation of the glacier's melt, resulting in a correlation coefficient of 0.83.

The mean annual mass balance of the Mandrone Glacier over the 1995-2006 period results in an average water equivalent net loss of 1290 mm a^{-1}, with a maximum value of 319 mm for the 2000/01 balance year and a minimum value of –3050 mm for the 2002/03 year.

KEY WORDS: Glacier retreat, Mass balance, Energy balance, Mandrone Glacier, Southern Central Alps.

RIASSUNTO: RANZI R., GROSSI G., GITTI A. & TASCHNER S., *Bilancio energetico e di massa del Ghiacciaio del Mandrone (Adamello, Alpi Centrali).* (IT ISSN 0391-9838, 2010).

Il ghiacciaio dell'Adamello, l'area glacializzata più estesa della Alpi Italiane, consiste di cinque unità idrografiche, la più grande della quali è il ghiacciaio del Mandrone che ricopriva una superficie di 13.38 km^2 nel giugno del 2003.

Al fine di valutare il bilancio di massa annuale del ghiacciaio del Mandrone, è stato applicato il modello di bilancio energetico PDSLIM: un modello stagionale di bilancio energetico e di massa del manto nevoso e delle superfici glaciali, di tipo distribuito e che suddivide il manto nevoso ed i ghiaccio in due strati. In questa memoria vengono descritti il modello di bilancio energetico e il sistema di monitoraggio idrometeorologico utilizzato per le simulazioni e la loro verifica. A grande scala, dal confronto dell'estensione del manto nevoso simulata dal modello con quella classificata da immagini satellitari è risultata una corrispondenza dell'86%. I volumi di deflusso misurati alla sezione di chiusura del bacino del Sarca di Genova alla stazione di Ponte Maria per un periodo di dodici anni (1995-2006) sono stati utilizzati per verificare la simulazione della fusione del ghiacciaio. Il confronto dei volumi di deflusso con la fusione del ghiacciaio ha dato buoni risultati, con coefficiente di correlazione pari a 0.83.

Il bilancio di massa medio annuo del ghiacciaio del Mandrone nel periodo 1995-2006 denuncia una perdita media netta di equivalente in acqua di 1290 mm a^{-1}, con valori di bilancio di massa compresi tra il massimo di 319 mm per l'anno 2000/01 ed il minimo di –3050 mm per l'anno 2002/03.

TERMINI CHIAVE: Ritiro dei ghiacciai, Bilancio di massa, Bilancio energetico, Ghiacciaio del Mandrone, Alpi Centrali.

INTRODUCTION

In the last decades a great attention has been devoted to the analysis of the global climate and the potential impact of its change on the hydrosphere and the cryosphere (IPCC, 2007). Glacial retreat, observed worldwide since the first decades of the 19th century at the end of the Little Ice Age, together with its recent acceleration (WGMS, 2008; Paul & *alii*, 2004), is one of the most remarkable signs of global warming. In most cases a variation in the physical characteristics (e.g. area, thickness, radiative pro-

(*) *Università di Brescia, Dipartimento di Ingegneria Civile, Architettura, Territorio e Ambiente, Via Branze 43 - 25123 Brescia, Italy*
ranzi@ing.unibs.it

This research was funded by the University of Brescia through the grant MURST ex 60% 2001-2008 «Monitoring of Glaciers», by the PRIN 2008 grant and by Fondazione CARIPLO within the research project «CARIPANDA» coordinated by Parco dell'Adamello. Parco Adamello-Brenta is gratefully acknowledged for having authorised the installation of the meteorological station of the University of Brescia at Passo della Lobbia Alta. Meteorological and runoff data were available thanks to ENEL, Meteotrentino, Provincia Autonoma di Trento (Servizio Opere Idrauliche) and Arpa Lombardia. Several students and alpine guides contributed to the field campaigns: their enthusiam and help motivated and supported our work. R. Ceschini and A. Collini are thanked for their logistic and moral support during our eight year long field surveys.

Two anonymous reviewers are thanked for their comments.

perties, water content, temperature, debris cover) of a glacier is an index of a changing climate, as clearly indicated by conceptual models and supported by measurements reported in several studies (see for example Kuhn, 1979; Ohmura & *alii*, 1992). This is one of the reasons for an increasing interest in the monitoring and modelling of glacier dynamics worldwide and on the documentation of "signatures" of global warming that can result from investigations on the cryosphere.

Focusing on the Southern Alps, a retreat of the Italian Alpine glaciers has been observed on average since the beginning of the 1980s (Santilli & *alii*, 2002; Baroni & Carton, 1990; Calmanti & *alii*, 2007), at a greater velocity in the eastern and central areas than in the western area. Terminus fluctuations show that Italian Alpine glaciers underwent a generalised retreat during the 20th century with one readvance episode in the 1970s and a poorly documented one around the early 1920s (Citterio & *alii*, 2007). Mass balances evaluated through the glaciological method (Kaser & *alii*, 2003), have been estimated in Italy systematically since 1967 on the Caresèr Glacier (Zanon, 1992; Giada & Zanon, 1996) and are still performed there today (Carturan & Seppi, 2007). For other mid-size glaciers, some of them close to the Adamello group, shorter time series are available (see e.g. Diolaiuti & *alii*, 2002, Kaser & *alii*, 1995).

The objective of this study is to assess the mass balance of the largest glacierised area of the Southern Alps: the Adamello glacier. It is known (Kuhn & *alii*, 1985) that the response of a glacier to climate fluctuations depends on its specific geomorphological characteristics, such as topography, aspect, hypsometry and glacier surface conditions including the debris cover. Then, because of its geomorphological difference compared to midsize glaciers for which mass balances are available, the Adamello glacier can be considered as a representative example of large glaciers in the same climatic subregion of the Alps as identified by Auer & *alii* (2007). Observations and modelling of its mass balance variability can therefore be useful for investigating the features of the response of glaciers to climate fluctuations in the southern Alps and the impact of such changes on runoff, sediment transport, local microclimate and landscape.

Because of its large size and complex logistic it is difficult to estimate the mass balance of the Adamello Glacier by using the glaciological method, and no systematic, long term measurements of mass balance have been conducted so far, although its changes in area and its terminus retreat over the last two centuries are well documented (Marchetti, 1978-1993; Baroni & Carton, 1990; Marchetti, 1999-2004; Maragno & *alii*, 2009), marking a 200 m retreat during the 1953-2002 period. For this reason an alternative approach was followed in the analysis reported in this work: an energy balance physically-based and distributed model was applied to assess the seasonal and annual mass balance of the Mandrone Glacier, the major glacial unit of the Adamello Glacier, drained by the Sarca di Genova river. To this aim meteorological, hydrological and glaciological data from 1995 to 2006, were collected and processed, as described in the second section. Then the energy-balance model and the resulting mass balance computation is presented in the third section. The annual mass balance was then estimated for each of the twelve years and discussed as reported in the last two sections of the paper.

THE STUDY AREA AND THE HYDROMETEOROLOGICAL DATA

The Adamello and Mandrone Glaciers

The Adamello massif, with a maximum altitude of 3539 m a.s.l., is located in the eastern part of the Central Italian Alps. Its slopes, including the Adamello Glacier, belong to two different administrative regions: the Lombardia region (specifically the province of Brescia) and the Trentino-Alto Adige/Südtirol region (specifically the province of Trento). Fig. 1 shows the boundaries of the study area and the location of some of the meteorological stations and the two hydrometric monitoring sites used for our analysis.

At the end of the 19th century, as reported by Payer (1865), some authors considered the Adamello Glacier as a single glacier, consisting of one accumulation zone and several effluences radiating out in the respective valleys. If we still consider the Adamello Glacier as a unique connected glacial unit (as for instance in S.G.L., 1992), the area of its glacierized surface is the widest in Italy (Baroni & Carton, 1996). It measures 17.24 km^2 according to the analysis of the ASTER satellite image scanned on the 20th of June 2003. The official Italian Glacier's Inventory (Comitato Glaciologico Italiano - C.N.R., 1961) divides the glacier into six units: the Pian di Neve plateau and the Miller Superiore, Salarno, Adamé, Corno di Salarno and Mandrone glaciers effluences, located in four separate valleys. The mass balance study presented here is focused on the Mandrone Glacier, the major hydrographic unit, coded as I-4L01011-15 in the World Glacier Inventory, which generates the major source of the Sarca di Genova river: its area measures 13.38 km^2 as estimated from the 20th of June 2003 image, and taking into account the ice flow direction observed over Pian di Neve and the glacier's divide identified by Baroni and Carton (1996). It can be considered as a valley glacier (C.G.T., 1994) with a north-east facing tongue, and altitude ranging from 2586 m a.s.l. to 3406 m a.s.l., as detected from the ASTER image superimposed on a digital elevation model. The mean altitude of the glacier was about 3040 m a.s.l. in summer 2003. The glacier is surrounded by high mountains as Monte Adamello, Punta Venerocolo and the Lobbia Alta peaks, shown in fig. 1.

In the scientific literature several studies are reported dealing with the Adamello Glacier. Pioneer field surveys were carried out by Julius Payer in 1864 and published one year later (Payer, 1865). Since then, after the end of the Little Ice Age, the glacier has been monitored, with increasing intensity in the second decade of the last century. The terminus retreat has been monitored on a continuous

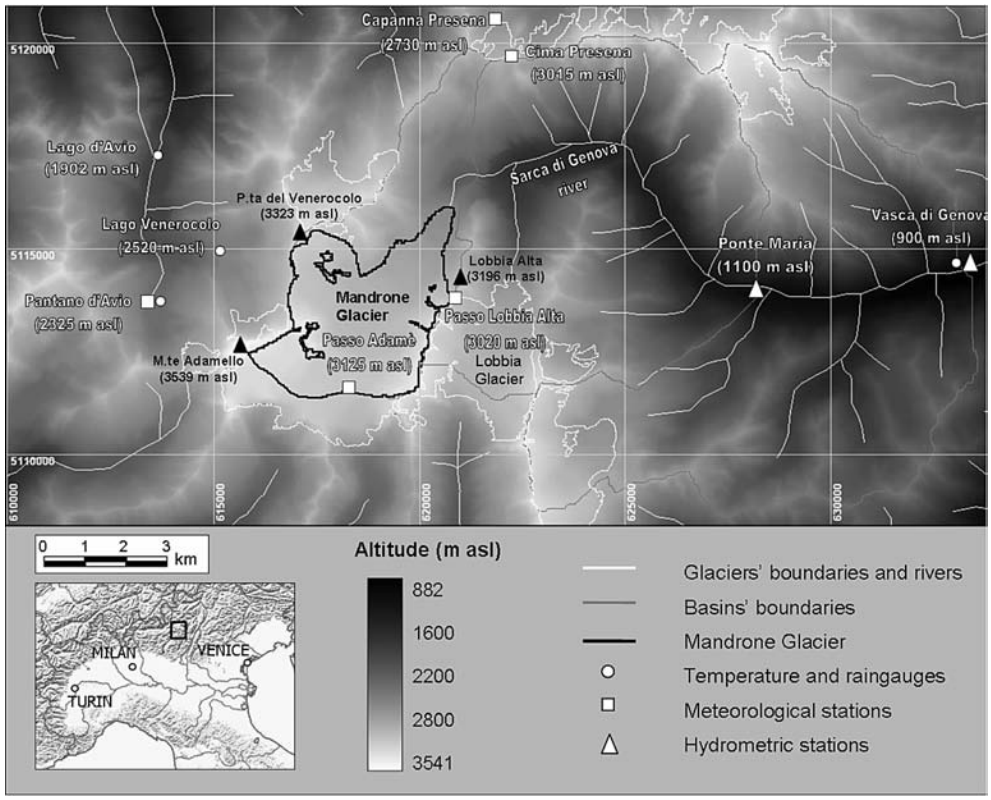

FIG. 1 - Val di Genova map on the UTM coordinates grid: the hydrological basins (light grey) and the glacier's boundaries (white line) are outlined, together with the two hydrometric (white triangles) and the nearest meteorological stations (white squares). The Mandrone Glacier boundaries are in black. Black triangles indicate major mountain peaks surrounding the glacier.

basis (Marchetti, 1978-1993; Marchetti, 1999-2004) until today and data archived by the WGI. A first estimate of the glacier thickness by using geophysical methods was provided on the basis of seismic observations by Carabelli (1961) who estimated a maximum thickness of 260 m; Astori & Togliatti (1964) used aerial photogrammetry to produce a detailed topograpic map with 5 m interdistace in altitude. Other works by Baroni & Carton (1990, 1996) and Baroni & *alii* (1992) were mainly focused on the reconstruction of the glacier variations in the past using different methods. Recent studies by Frassoni & *alii* (2001) provided measurements with georadar of the Adamello Glacier's thickness, which ranged in the 1997 and 1998 years from a maximum depth of 240 m in the Pian di Neve area close to Passo Adamè to 50 m in the tongue close to the terminus; Ranzi & Taschner (2005) estimated snow, firn and ice albedo with satellite images and in situ measurements and Baroni & *alii* (2004) investigated the permafrost environment in the surrounding areas. Recently Maragno & *alii* (2009) documented changes of the areal extent of the Adamello glacier, compared to the ongoing decline of Alpine glaciers.

METEOROLOGICAL AND SNOW MEASUREMENTS

Meteorological and snow monitoring over the study area was actually conducted after a critical analysis and processing of meteorological and hydrometric data provided by a network of gauges in the surrounding area (about 800 km^2) of the Adamello Glacier (see fig. 2): data from 17 meteorological stations and 15 snow depth and density measurement points were processed altogether over the 1995-2006 monitoring period. Most of the monitoring sites are located at an intermediate altitude, i.e. between 900 and 2000 m a.s.l., but several others are located at a high altitude, over 2000 m a.s.l. As the hypsometry of the glacier ranges from about 2600 to 3400 m a.s.l., great attention is paid to a proper description of the physical processes and meteorological variables occurring at high elevations. At this aim meteorological measurements referring to high altitude sites as close as possible to the Mandrone Glacier were selected to drive the model simulations.

For the 1995 and 1996 ablation seasons, air temperature, humidity, wind speed, incoming radiation and atmospheric pressure data recorded at the meteorological station installed by ENEL on the glacier at Passo Adamè (3150 m a.s.l.) were assumed to be representative of the Mandrone glacier's conditions. As this station was later no more in operation, for the 1997 to 2000 period, the most representative monitoring site was assumed to be the Cima Presena station, located at 3015 m a.s.l. on a peak close to the glacial environment. In the following six-years period the meteorological information required to simulate the glacier energy and mass balance was mainly provided by the automatic weather station installed at Passo della Lobbia Alta (3020 m a.s.l., see fig. 1) on the 9th of August 2001. At that time the station was based 3 m deep in the snow accumulated on the top of the Lobbia glacier (see fig. 3) and a

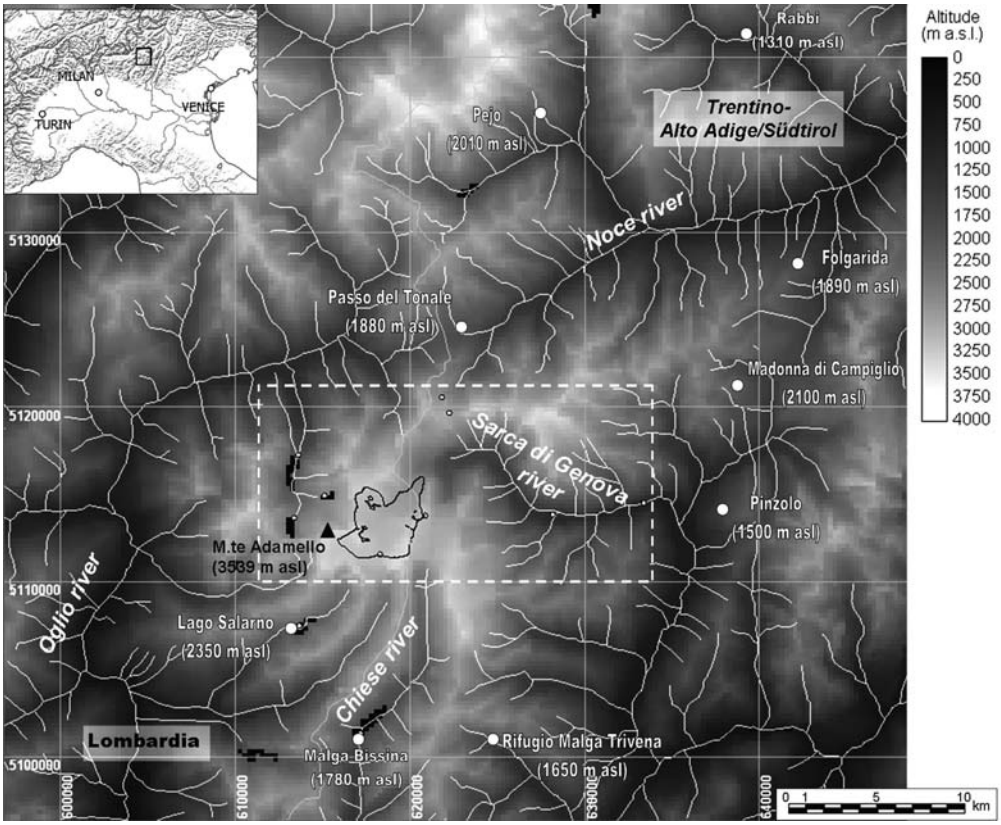

FIG. 2 - The meteorological monitoring network: the white rectangle is zoomed in fig. 1.

few tens of metres away from the Mandrone glacier. Ice was found at the bottom of the basement at the time of the installation, but in the successive years both the Lobbia and the Mondrone glaciers retreated some tens of meters far from the station. The Passo della Lobbia station measured air temperature and humidity, wind speed and direction, net shortwave and longwave radiation with LSI-LASTEM instruments and shortwave incoming and reflected global radiation with a Kipp & Zonen albedometer. Even if in the following years the Lobbia glacier retreated from the station's site, this site is still considered a good reference for the meteorology of the investigated area because of its altitude, its location between two glaciers and because of the local winds and radiation conditions.

FIG. 3 - The Passo della Lobbia Alta (3020 m a.s.l.) meteorological station. Wind speed and direction, air temperature and humidity, incoming and reflected global radiation and net radiation are measured. The photograph was taken on the 17th of August 2001, eight days after the installation. On the right: Crozzon di Lares peak (3354 m a.s.l.).

Only when missing data were present, the surrounding stations of Cima Presena, Capanna Presena (2730 m a.s.l.), also close to a glacier, Pantano d'Avio (2325 m a.s.l.) and Passo del Tonale (1880 m a.s.l.) were used. The correlation of data from the surrounding stations with respect to those at Passo Adamè and Passo della Lobbia Alta was used to estimate meteorological conditions representative for the glacier. Missing temperature data were estimated on the basis of a temperature lapse rate computed from the network of surrounding stations. Temperature data recorded at Cima Presena have a linear correlation coefficient with the Passo della Lobbia data in the range 0.94-0.96 and a bias of ±0.2 °C at 0°C. Also radiance, wind speed and humidity data of Cima Presena were close to the Passo della Lobbia data. The hourly air temperature recorded at Passo della Lobbia Alta during the month of August, which is the most relevant for the energy balance as the highest ablation occurs, is plotted in fig. 4: data start from year 2001, when the meteorological station was installed. For the year 2004 and for the days prior to the station's installation on the 9th of August 2001 data were reconstructed after the Cima Presena hourly data. Signifi-

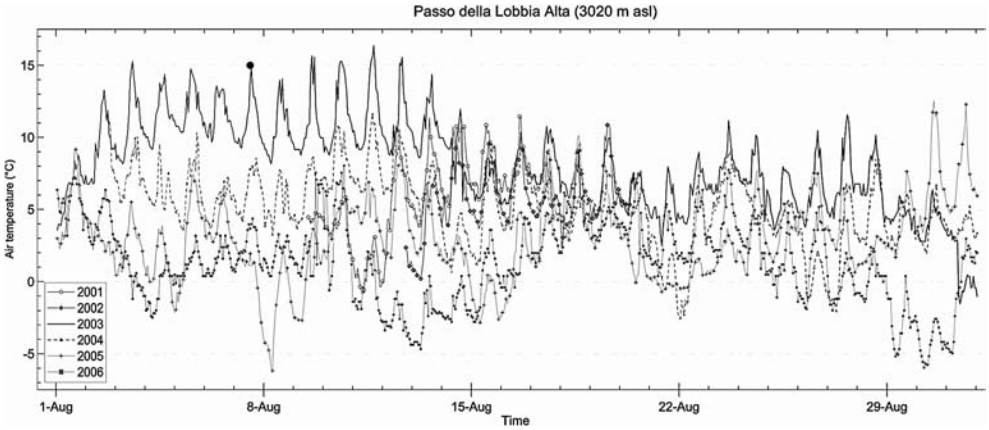

FIG. 4 - Hourly air temperature recorded in the month of August at Passo della Lobbia Alta (2001 to 2006 years). On the 7th of August 2003 a temperature value of 15°C (black circle) was measured at 12:00 local time (CET) at the station. For the rest of August 2003 and some missing values in the other years data, e.g. in August 2001 before the 9th of August, data were reconstructed with values recorded at Cima Presena (3015 m a.s.l.) station.

cant inter-annual differences, up to 15 °C, can be noticed and the extremely hot temperatures of the 2003 summer are evident from the data. Mean annual and monthly temperatures estimated at the site of the Passo della Lobbia Alta station are reported in tab. 1.

Precipitation recorded at Passo del Tonale or at Vasca di Genova (the closest station in the Sarca riverbasin, at 900 m a.s.l. altitude) was assumed as a reference, but a correction factor was applied as altitudinal precipitation gradients were observed in the surrounding area. In fact, thanks to measurements conducted with a precipitation totaliser until the 1970s, a mean annual precipitation of 1421 mm was measured at 2441 m a.s.l., two kilometres apart from the Mandrone glacier, over the 1963-1972 period. An annual precipitation lapse rate Γ_p=0.312 mm m^{-1} and a reference annual precipitation at sea level estimated as P_0=717 mm (over a dense network which was available in that period at high altitudes) were applied to correct precipitation data in our simulations, assuming an altitudinal linear trend and a multiplicative correction factor as in Ranzi & *alii* (1999). See also Beniston (1997) Brunetti & *alii* (2000), Laternser & Schneebeli (2003) for reference on this issue.

Incoming global shortwave radiation data were used in input to the energy balance model. Net radiation and reflected shortwave global radiation data, collected over the 2001 to 2006 period at the Passo della Lobbia Alta meteorological station, were used to validate the net shortwave and longwave radiation components of the energy balance model, described in the next section.

Surface properties of the Mandrone glacier were surveyed by field investigations throughout the 2001-2008 pe-

TABLE 1 - Mass balance of the Mandrone Glacier (1995-2006) and hydrological regime of the Sarca di Genova basin. The mean annual mass balance of –1290 mm results as the sum of the winter mass balance estimated as the April 1st snow water equivalent (673 mm) and the summer glacier's mass balance (–1963 mm)

		J	F	M	A	M	J	J	A	S	O	N	D	Sum/ Mean
Mandrone Glacier[1]	Rain on snow r (mm)	–	–	–	0	9	47	44	43	22	–	–	–	**166**
	Snowfall s (mm)	–	–	–	150	135	73	35	54	64	–	–	–	**513**
	Sublimation from ice e_{ice} (mm)	–	–	–	0	0	–1	–5	–8	2	–	–	-	**-12**
	Snow evaporation e_{snow} (mm)	–	–	–	20	22	21	13	7	9	–	–	–	**91**
	Ice melt m_{ice} (mm)	–	–	–	0	0	97	426	594	252	–	–	–	**1368**
	Snowmelt m_{snow} (mm)	–	–	–	0	88	538	371	140	53	–	–	–	**1190**
	Snow water equivalent (1st day of the month) (mm)	–	–	–	**673**	803	837	398	93	43	67	–	–	
	Glacier's mass balance b (mm)	–	–	–	**130**	**34**	**-535**	**-726**	**-636**	**-230**	–	–	–	***-1963***
	Rain on ice r_{ice} (mm)	–	–	–	0	0	9	38	55	13	–	–	–	**115**
	Total precipitation p (mm)				150	144	129	117	152	99				**791**
	Mean monthly temperature at Passo della Lobbia[2] (°C)	-10.2	-10.2	-8.5	-6.3	-1.2	2.3	4.2	4.0	0.9	-1.3	-7.0	-9.4	**-3.5**
Sarca di Genova	Runoff at Ponte Maria[3] (mm)	–	–	–	62	203	330	369	316	167	112		–	**1559**
	Runoff at Ponte Maria[3] (m^3/s)	–	–	–	1.85	5.87	9.88	10.69	9.14	4.98	3.25		–	**6.54**
	Corrected precipitation[4] (mm)	87.5	63.6	81.6	168.5	122.3	151.7	149.4	115.5	168	210.7	165.7	116.5	**1601**
	Runoff at Vasca di Genova[4] (mm)	9.3	14.3	22.6	60.7	184.4	253.2	288.0	237.5	128.9	63.1	31.3	52.1	**1345**
	Runoff at Vasca di Genova[4] (m^3/s)	0.48	0.82	1.17	3.24	9.53	13.52	14.88	12.27	6.88	3.26	1.67	2.69	**5.90**

[1] Area 13.38 km^2.
[2] Station altitude 3020 m a.s.l.. Missing data (e.g. in the period 1995-2000) are interpolated from surrounding stations after estimating the temperature lapse rate.
[3] Basin area 77.52 km^2. Observation period (1995-2006).
[4] Basin area 138.4 km^2. Observation period (1989-1996).

riod. The objective was to observe the glacier's surface and the position of the transient snowline and the firn and measure some physical properties of snow and ice, relevant for the energy balance model, such as albedo and snow density. A detailed field survey was carried out during the summer of 2002 on the Adamello Glacier, aimed at monitoring the physical characteristics of the snow and estimating the albedo in several sites. On the 19th and the 20th of August 2002, air temperature, incoming and reflected radiation were measured, together with temperature, density, liquid water content, shape and size of the snow grains in six different sites. Other snow density measurements were conducted in the following years. Seasonal snow density ranged, on average, between 300 kg m^{-3} in June and 510 kg m^{-3} in August. Point albedo measurements of seasonal snow at four different sites were in the 0.4-0.5 range, while ice surface reflected from 20% to 30% of incoming radiation.

Streamflow Measurements

The hydrometric station located at Ponte Maria at 1100 m a.s.l. altitude, (fig. 1 and fig. 5) records the water level of the Sarca di Genova river, downstream the glacier, gauging a drainage area of 77.52 km^2, 25% glacierised. A second downstream measurement station named Vasca di Genova is located at the intake of a sedimentation basin of a hydropower system at 900 m a.s.l. altitude and draining an area of 138.4 km^2, 18% glacierised.

For the gauged section of Ponte Maria we carried out seven discharge measurements in the period 2001-2005 (tab. 2) to calibrate a stage-discharge rating curve (fig. 6). A power-law analytical expression, as widely used in the hydrological practice for the discharge rating curve, was adopted:

$$Q = a \cdot (h - h_0)^b, \quad (1)$$

where Q (m^3/s) is a function of the water level h (m), measured with a CAE ultrasonic hydrometer, h_0 is a reference level (m) and a and b are calibration parameters. The best

Table 2 - Discharge measurements at the Sarca di Genova at Ponte Maria hydrometric station (1100 m asl) in the period 2001-2005. On the 12th december 2005 the stream was partially frozen

Date and time	Water level	Discharge	Area	Velocity		
				mean	surface mean	surface maximum
	(m)	(m^3/s)	(m^2)	(m/s)	(m/s)	(m/s)
03/06/2001 12:25 - 16:40	0.75	6.2	7.0	0.89	1.10	1.77
18/08/2002 14:20 - 16:20	0.78	7.8	8.4	0.93	1.24	1.74
18/8/2005 10:30 - 12:25	0.67	5.2	7.5	0.69	0.8	1.7
18/8/2005 14:30 - 15:45	0.89	12.3	12.1	1.01	1.31	3.15
19/8/2005 08:00 - 09:30	0.61	5.1	6.5	0.79	0.97	1.77
04/11/2005 10:45 - 12:30	0.38	1.5	3.7	0.4	0.47	0.812
12/12/2005 13:30 - 14:50	0.37	0.8	1.8	0.46	0.51	1.18

Fig. 5 - Ponte Maria hydrometric station (1100 m a.s.l.), with the staff gauge on the right bank of the bridge and the ultrasonic hydrometer in the centre.

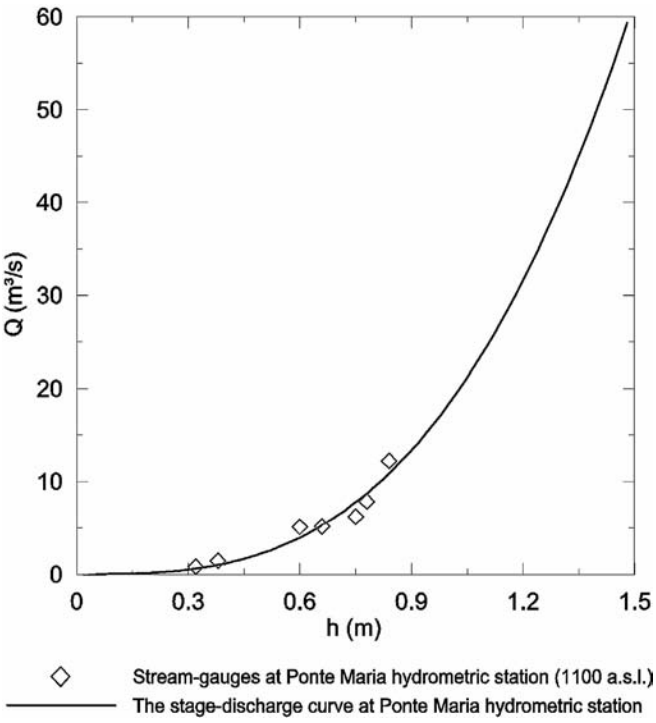

Fig. 6 - The stage-discharge curve for the Ponte Maria hydrometric station.

fit of measurements was obtained assuming a=18.317, b=2.996, h_0=0 m. Before the 19th September 1999, when a flood carrying coarse debris and gravels raised the level of the cross section, the reference level h_0 was set to –0.05 m, so that early spring runoff before that period was in agreement with the mean values of the following period. The high value of the b exponent reflects the shape of the cross section, including a lateral by-pass channel receiving water in excess of a threshold level of about 0.7 m.

The reconstruction of the mean hydrological regime at Sarca di Genova was possible thanks to the availability of raingauge data and runoff measurements at the intake of the Vasca di Genova reservoir over the 1989 to 1996 period. Daily data at Vasca di Genova support the verification of the accuracy of the stage-discharge rating curve at the Ponte Maria hydrometric station, as fig. 7 shows.

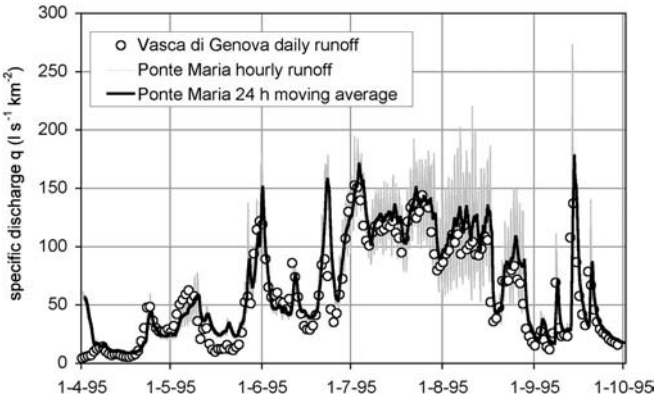

FIG. 7 - Comparison between the hourly specific discharge at the Ponte Maria hydrometric station (altitude: 1100 m, area: 77.52 km^2) and the daily discharge measured at Vasca di Genova (altitude: 900 m a.s.l., area: 138.4 km^2).

It has to be considered, however, that the Vasca di Genova inflow underestimates the Sarca di Genova runoff because environmental flow is released downstream the basin and large floods are not measured. As represented in fig. 7, the amplitude and the timing of the hourly specific runoff measured for the Sarca river at Ponte Maria and the daily runoff measured at Vasca di Genova are in good agreement. The runoff regime of Sarca di Genova is of the glacial type, with a single maximum in summer and a high correlation with mean monthly air temperature. A different behaviour is shown by the precipitation regime, with areal precipitation estimated with Thiessen polygons and taking into account systematic measurement errors and altitudinal precipitation gradients as described in Ranzi & *alii* (1999). Two precipitation maxima occur, a major one in autumn and a second one in spring (fig. 8 and tab. 1). The runoff coefficient of the basin, i.e. the ratio between annual runoff and precipitation, is 83%.

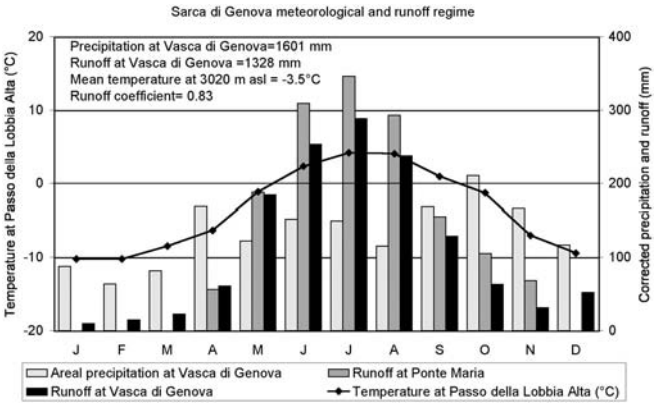

FIG. 8 - Sarca di Genova hydrological regime at the Ponte Maria (1995-2006 years) and Vasca di Genova (1989-1996 years) runoff stations, and mean monthly air temperature reconstructed at Passo della Lobbia Alta (1995-2006 years).

SATELLITE MONITORING

Because of the areal extension of the Adamello Glacier and the wide spatial variability of the radiative properties of its ice, firn and seasonal snow cover, satellite images characterized by high spatial resolution are of fundamental importance to estimate maps of albedo and to monitor temporal and spatial variability of transient snow covered areas.

To achieve these objectives ASTER images scanned from the TERRA satellite were chosen on a cost-efficiency basis. These images were made available within the GLIMS project (Kargel & *alii*, 2005). The 15 m spatial resolution of these images permits to obtain detailed albedo maps of the snow cover and the ice surface, suitable for the available DEM resolution. The radiative module implemented in the energy balance model, including a sun-tracking algorithm to compute shadowed areas and incident direct radiation, the computation of direct and diffused radiation from the sky and the surrounding terrain and a spectral atmospheric attenuation model derived from literature data were used to simulate distributed incident radiative flux. With the radiance reflected by the surface to the sky measured by the satellite-borne ASTER sensor on the 23rd of August 2003 image and assuming an atmospheric albedo of 0.07, a distributed albedo map was derived. Over the ice covered areas the mean reflectivity was 0.5, while the snow patches still present in late August reflected 83% of incoming radiation. The slightly higher albedo of ice we estimated, compared to that assumed by Klok & Oerlemans (2002) for the Morteratschgletscher, in Switzerland, can be explained by the fact that ice crusts and crystals are often observed on the Mandrone ice surface, possibly because of frequent sublimation and evaporation cycles. Snow albedo values are in agreement with literature data and with in situ measurements.

Typically albedo values of ice surfaces are marked out by a higher spatial variation and a lower temporal variation than snow covered areas; for example, the presence of de-

bris cover over a glacier decreases the value of the albedo, while ice crusts, which form as a result of sublimation and evaporation and are often observed over the Mandrone glacier, increase the value of albedo, if compared with values over pure ice. Snow albedo is characterized by a higher temporal variability, that is, albedo values can change by 30% in a few days. For example, albedo values measured at Passo della Lobbia Alta, from the 26th of May, just after a spring snowfall, up to the 6th of June of 2005, varied from 0.85, a typical value for fresh snow, to 0.55 a typical value for wet snow. One station installed on the Mandrone glacier in the summer of 2008 measured ice albedo in the 0.3-0.5 range and fresh snow albedo in the 0.7-0.9 range. In the model, while ice albedo is assumed as a distributed map derived from the satellite image, and constant in time, the distributed snow albedo is assumed to change according to a model described in Ranzi & Rosso (1991) which takes into account season, snow metamorphosis and diffused radiation.

METHODS

Annual mass balance

Among the different methods to assess the mass balance of a glacier, when the access to large glaciers is difficult for the glaciological method to be adopted, the hydrological method can be a valid alternative. It implies the estimation of outgoing and incoming water volumes to the glacier over a given period, typically one year or the accumulation and the ablation seasons. In order to properly evaluate the outgoing mass, a reliable estimate of snowmelt and icemelt is necessary and the application of a distributed energy balance model can be adopted. Runoff measurements can also be conducted for verification.

For each of the twelve hydrological years 1995-2006 the annual mass balance of the Mandrone Glacier, expressed in terms of equivalent water volume B [L^3], was estimated as the sum of the winter balance and of the summer balance, each lasting six months. For a given hydrological year, it is assumed that winter starts on the 1st of October, denoted as t_{0w}, of the previous year and ends on the 31st of March, denoted as t_{fw}, of the current year. The ablation season starts, in our working assumption, on the 1st of April, $t_{0s} = t_{fw}$, of the balance year, when the first spring snowmelt episodes are detected in some years on the hydrograph at the Ponte Maria hydrometric station (see for instance fig. 7), and ends on the 30th of September, t_{fs}, of the balance year. For the Mandrone Glacier's surface, A_g, outlined in fig. 1 and assumed to have a constant area of 13.38 km^2 over the twelve year simulation period, the mass balance B is computed as the sum of the balance of the snow-covered areas changing in time, $A_{snow}(t)$, and that of the firn- or ice-covered areas, assumed as a single unit, with area $A_{ice}(t)$, also changing in time. The total glacier's area is then constant and equal to $A_g=A_{snow}(t)+A_{ice}(t)$.

Winter mass balance

The winter glacier's mass balance, B_w, is estimated as the sum of the firn and ice mass balance and of the snow mass balance. The firn and ice winter mass balance, $B_{w,ice}$, is assumed to be equal to the total volume of the snow water equivalent left at the beginning of the balance year, $S_{weq}(t_{0w})$, which starts its metamorphosis into firn and later ice. Ice melt is assumed to be negligible in winter. The snow winter mass balance, $B_{w,snow}$, is given by the difference, $S_{weq}(t_{fw}) - S_{weq}(t_{0w})$, between the snow water equivalent measured at the end, $S_{weq}(t_{fw})$, and that simulated at the beginning of the winter period, $S_{weq}(t_{0w})$, the last often being small or negligible. The snow water equivalent on the 1st of April of each year is estimated by interpolating with a logistic curve the snow water equivalent measurements available from a network of about fifteen stations available in the domain of fig. 1 up to an altitude of 2700 m. As a result, the glacier's winter mass balance is:

$$B_w = B_{w,ice} + B_{w,snow} = S_{weq}(t_{0w}) + S_{weq}(t_{fw}) - S_{weq}(t_{0w}) = S_{weq}(t_{fw}). \quad (2)$$

This assumption is consistent with the literature (see for instance Ohmura & *alii*, 1992).

Summer mass balance

Over the snow-covered areas the snow mass balance, $B_{s,snow}$, with dimension [L^3] is computed as the sum of the point mass balance over each pixel of the domain, measuring dA=30 m x 30 m= 900 m^2:

$$B_{s,snow} = S_{weq}(t_{fs}) - S_{weq}(t_{0s}) =$$
$$= \int_{t_{0s}}^{t_{fs}} \int_{A_{snow}(t)} [r(A(t),t) + s(A(t),t) - m_{snow}(A(t),t) - e_{snow}(A(t),t)]\,dA\,dt \,. \quad (3)$$

where r represents the rainfall rate, s is the snowfall, m_{snow} is the snowmelt (including drainage of the snow liquid water content) and e_{snow} represents net snow evaporation and sublimation losses. All these terms have dimension [LT^{-1}]. Because rainfall over firn and ice areas is assumed to flow as runoff on the surface and in subsurface channels of the glacier the summer balance $B_{s,ice}$ of this part of the glacier, with area $A_{ice}(t)$, is always negative being the sum of the melt rate, m_{ice}, and sublimation rate, e_{ice}, computed as:

$$B_{s,ice} = \int_{t_{0s}}^{t_{fs}} \int_{A_{ice}(t)} [-m_{ice}(A(t),t) - e_{ice}(A(t),t)]\,dA\,dt \,. \quad (4)$$

As a consequence, the summer mass balance of ice and snow over the glacier's area A_g is

$$B_s = \int_{t_{0s}}^{t_{fs}} \int_{A_g(t)} [p_{snow}(A(t),t) - m(A(t),t) - e(A(t),t)]\,dA\,dt \,. \quad (5)$$

Where p_{snow} represents total precipitation rate, either rain, r, or snow, s, over snow, $m=m_{snow+}\ m_{ice}$ the total melt, including drainage from the snowpack, and $e=e_{snow}+e_{ice}$ evaporation and sublimation from snow and ice, all terms having dimension [LT^{-1}] and negative sign when conden-

sation of air water vapour occurs. Total precipitation over the glacier, p, is the sum of total precipitatiom on snow, p_{snow}, and rain on ice, r_{ice} which does not contribute to the glacier's mass balance because it runs off the glacier's surface. The annual mass balance is given by the sum of the winter and summer mass balances:

$$B = S_{weq}(t_{fw}) + \int_{t_{0s}}^{t_{fs}} \int_{A_g(t)} [p_{snow}(A(t),t) - m(A(t),t) - e(A(t),t)] dA dt \quad (6)$$

The annual specific mass balance over a unit surface of the glacier, with dimension [L], can be obtained as:

$$b = \frac{B}{A_g} = \frac{B_{snow} + B_{ice}}{A_{ice} + A_{snow}} . \quad (7)$$

The basic terms of equations (1) to (6) are given in tab. 1, where they are reported with the same notation as above, but in units of volumes per unit surface of the glacier, that is expressed in millimetres of water equivalent over the computational period. Areal changes are neglected in our computation as their estimation would require a continuous monitoring of the glacier's areal extent.

Energy balance of snow and ice

In the following, the hypotheses of our energy balance modelling framework, called PDSLIM (Physically based Distributed Snow Land and Ice Model), are briefly described. This model is a development of the PDSM model, already applied at the catchment scale to simulate snowmelt in two alpine basins, Cordevole (Ranzi & Rosso, 1991) and Toce (see Grossi & Falappi, 2003 where the model's transpiration component is described). At the point scale the temperature and liquid water content dynamics of the snowpack model were verified with microwave radiometry during the MASMEX experiment, in the Cordevole test-site (Cagnati & *alii*, 2004; Macelloni & *alii*, 2005). The adaptation of PDSM to simulate the energy balance of glacierised basins was already tested for the debris-covered Belvedere Glacier (Ranzi & *alii*, 2004).

For a unit area and finite depth layer of ice or snow superimposed over ice, the melt rate can be computed from the energy balance equation

$$H_m + H_c = S_{io} + L_{io} + H_l + H_s + H_p + H_g , \quad (8)$$

where the terms, with units W/m^2, represent, respectively:

H_m: energy available for melt,
H_c: internal energy of the ice or snow layer,
S_{io}: net shortwave radiation,
L_{io}: net longwave radiation,
H_l: latent heat,
H_s: sensible heat,
H_p: advective heat from precipitation,
H_g: conductive heat at the bottom surface of the ice or snow layer.

For an ice or snow layer with finite depth Δz, specific heat C, density ρ and mean temperature T, thermal energy changes over time, t, with a rate

$$H_c = C \rho \Delta z \, dT/dt . \quad (9)$$

The specific heat of ice is set to $C=C_i=2093.4$ J kg^{-1} K^{-1} and its density is assumed $\rho=\rho_i=830$ kg m^{-3}, a literature value for firn (Paterson, 2004) which can be adopted also for ice at the surface, where ice porosity is high. The relatively low ice density, close to literature values for firn, was adopted because ice crusts and sublimation crystals were often observed on the glacier's surface, resulting on higher porosity. For snow, instead, density $\rho=\rho_s$ changes over time according to the snowpack simulation model already described in Ranzi & Rosso (1991) and Cagnati & *alii* (2004). Details of the computation of the shortwave and longwave radiation terms of the equation, S_{io} and L_{io}, after global shortwave radiation measurements, R_m, are basically those reported in Ranzi & Rosso (1991; 1995). In the application to glacierised areas, the diffused shortwave radiation from the sky, computed as R_d, and the fraction of the measured incoming global radiation, R_m, reflected by the terrain surrounding each point with average albedo $\alpha_t(x,y)$ contribute to the flux of diffused radiation at each point, $R_d(x,y)$. Considering the sky view factor, V_s, i.e. the fraction if the sky hemisphere surrounding each point, and the terrain view factor, V_t, which is its complementary value $V_t=1-V_s$ the diffused radiatio $R_d(x,y)$ results:

$$R_d(x,y) = R_d V_s(x,y) + \alpha_t(x,y) R_m V_t(x,y) . \quad (10)$$

Turbulent heat fluxes of sensible and latent heat (see for instance Hock & Holmgren, 2005; Denby & Greuell, 2000), H_s and H_l respectively, are computed according to the mixing length theory, assuming stable conditions at the snow and ice surfaces. This is a reasonable hypothesis during the melt season, in the lack of more detailed measurements of the wind field and the turbulent structure which are known to be complex (Brock & *alii*, 2006; Smeets & *alii*, 1998, 2000), but are seldom measured in detail over glaciers. Accordingly H_s and H_l can be computed as:

$$H_s = \rho_a C_p D_h (T_a - T_s) , \quad (11)$$

$$H_l = L_v \rho_a D_w \frac{0.622}{p} (e_a - e_s) , \quad (12)$$

$$D_h = D_w = \frac{k^2 u_z}{[\ln(z/z_0)]^2} , \quad (13)$$

being D_h, D_w turbulent heat and momentum exchange coefficients and
ρ_a (kg m^{-3}): air density,
C_p (J kg^{-1} K^{-1}): specific heat of air,
p (Pa): atmospheric pressure,
T_a (K): air temperature at height z,
T_s (K): ice or snow surface temperature,
e_a (Pa): air vapor pressure,

e_s (Pa): vapor pressure at the ice or snow surface,
L_v (J kg^{-1}): latent heat of sublimation.
u_z (m s^{-1}): wind velocity at measurement height z, assumed the same reference height for temperature and humidity,
z_0 (m): surface aerodynamic roughness,
k=0.4: Von Karman constant.

Surface roughness z_0 is assumed 0.007 m for ice after Hock (1998), while for snow it is 0.003 m (see for instance Plüss & Mazzoni, 1994). The measurement height z is 6 m in the case of the Passo della Lobbia meteorological station in late summer, when the seasonal snow is, generally, completely melted. When snow is present, according to measurements or simulations, the effective measurement height is computed as the distance between the height of the sensor and the snow surface depth simulated by the model. It is worth noticing that in the year the station was installed, 2001, 3 m of snow were still present in August (see fig. 3), the maximum value observed for that month over the 2001 to 2008 measurement period at that site.

Both air temperature and atmospheric pressure were estimated at each 30 m x 30 m grid cell of the glacier's Digital Elevation Model on the basis of the respective altitude gradients. No correction was applied to measured relative humidity.

Conductive heat, H_g, at the bottom of a surface ice or firn layer 0.1 m deep is computed according to the Fourier law:

$$H_g = K_t \, dT/dz \ . \tag{14}$$

with K_t the thermal conductivity of ice (W m^{-1} K^{-1}), determined after Paterson (1994) as a function of the mean temperature of the ice layer, T_i

$$K_t = 9.828 \exp(-0.0057 \, T_i) \ . \tag{15}$$

The surface ice or firn layer is assumed to exchange conductive heat with an underlying isothermal, semi-infinite, ice layer at constant 0°C temperature, T_g, a reasonable assumption for a temperate glacier in the melt season.

With this assumption, the conductive heat flux gained from the glacier over the time step $[t_k, t_{k+1}=t_k+\Delta t]$, by the surface ice layer, with mean temperature $T_{i,k}$ at the beginning of the time step, results:

$$H_g = 2\sqrt{\frac{C \, \rho_i K_t}{\pi \, \Delta t}}(T_g - T_{i,k}) \ . \tag{16}$$

Let a and c represent the constant terms

$$a = C\rho_i \, \Delta z/\Delta t \ , \tag{17}$$

$$c = 2\sqrt{\frac{C \, \rho_i K_t}{\pi \, \Delta t}} \ , \tag{18}$$

and H_k the heat flux

$$H_k = S_{io} + L_{io} + H_l + H_s + H_p \ , \tag{19}$$

computed at the beginning of each computational time step $[t_k, t_{k+1}]$ in a finite difference implicit scheme to solve in time the energy balance equation (8) for the finite volume of the surface ice layer assumed 0.1 m deep. Then, combining equations (9), (16), (17), (18) and (19), assuming first that H_m=0 we can solve equation (8)

$$H_c = H_k + H_g \ , \tag{20}$$

with respect to the unknown mean ice temperature, $T_{i,k+1}$, at the end of the computational time step:

$$a(T_{i,k+1} - T_{i,k}) = H_k - c(T_{i,k+1} + T_{i,k})/2 \ , \tag{21}$$

obtaining

$$T_{i,k+1} = [H_k + T_{i,k}(a - c/2)]/(a + c/2) \ . \tag{22}$$

If $T_{i,k+1}$ results higher than 0°C the ice temperature is set to 0°C and the surplus heat available for ice melt is

$$H_m = max(a \, T_{i,k+1}, 0) \ . \tag{23}$$

The surface ice temperature, T_0, which is needed to compute the radiative and convective terms of equation (8) at the successive computational time step, assuming a linear temperature profile within the ice layer, is set twice the mean ice layer temperature, $T_{0,k+1}=2 \, T_{i,k+1}$.

A similar numerical scheme is adopted to simulate conductive heat fluxes in the upper snow layer, 0.1 m deep, and at the bottom of the snowpack.

When the temperature of the ice or snow layer reaches 0°C, melt can occur at a rate m (m s^{-1}) computed by dividing the energy flux H_m by the latent heat of fusion of ice, L_f=334944 J kg^{-1}, and the water density, r_w, being r_w= 1002.28 kg m^{-3} at 0°C:

$$m_{ice/snow} = H_m/L_f/\rho_w \ . \tag{25}$$

RESULTS

Mass balance of the Mandrone Glacier

The time variability of the annual mass balance of the Mandrone Glacier is shown in fig. 9, where the time series

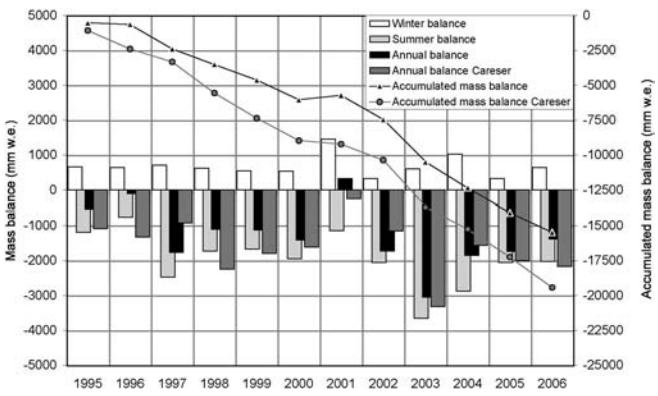

FIG. 9 - Mean winter, summer and annual mass balance and mean accumulated balance modelled for the Mandrone Glacier compared with the annual and accumulated measured mass balance of the Careser Glacier (Carturan & Seppi, 2007).

of the accumulated mass loss of about 15475 mm of water equivalent, estimated for the 1995-2006 balance years, is also represented. This corresponds to an estimated average mass loss of 1290 mm a^{-1} equal to the sum of the mean winter mass balance, 673 mm, estimated from equation (2) as the mean areal snow water equivalent on the 1st of April of each year, and the mean summer mass balance, given by equation (5) and reported in tab. 1 and tab. 3 and resulting in –1963 mm a^{-1}. The terms of equations (3), (4) and (7) computed for the ablation season are listed in tab. 1. The ablation rate during the ablation season strongly depends on the meteorological conditions occurring each year over the melting surface. In fact the boundary meteorological conditions induce a meaningful change in the value of the heat fluxes involved in the energy balance. With reference to the Mandrone Glacier and to the melting season, tab. 3 lists the mean annual and summer (from June to August) air temperature estimated at the site of the Passo della Lobbia Alta meteorological station, together with the winter, summer, annual and accumulated balance estimated over the twelve years (1995-2006). It is possible to observe, also from the data plotted in fig. 9, that for the year 2003, when the highest value of the mean summer temperature (6.7 °C) was recorded, the highest mean annual mass loss of 3050 mm of water equivalent was obtained. Conversely, the highest positive balance of 319 mm w.e., was obtained for the year 2001, owing to the highest initial mean water equivalent observed over the simulation period (1458 mm). This confirms an established consensus in the scientific literature, stating that key factors influencing mean annual net balance, b, are summer temperature T_{JJA} and winter balance b_w, (which is often assumed, as here, as the end of the winter snow water equivalent) summed to summer precipitation P (Ohmura & *alii*, 1992). The simple multiple linear regression equation:

$$b = -1258 - 473\, T_{JJA} + 1.123\, (b_w + P)\,, \qquad (26)$$

TABLE 3 - Mean annual and summer (from June to August) air temperature estimated at Passo della Lobbia Alta (3020 m asl), mass balances expressed in millimetres of water equivalent over the Mandrone Glacier. The Equilibrium Line Altitude and the Accumulation Area Ratio are reported. Maxima are in bold, minima in italic

Year	Annual air temperature (°C)	Summer air temperature (°C)	Winter balance (mm)	Summer balance (mm)	Annual balance (mm)	Accumulated balance (mm)	E.L.A. (m a.s.l.)	A.A.R. (-)
1995	-4.4	2.0	658	-1187	-529	-529	3173	0.183
1996	*-4.9*	*1.8*	642	**-754**	-112	-641	3086	0.530
1997	-3.8	2.7	711	-2475	-1764	-2405	3313	0.007
1998	-3.1	4.5	620	-1727	-1107	-3512	3300	0.025
1999	-3.5	3.2	545	-1667	-1122	-4634	3289	0.038
2000	-2.7	3.6	537	-1948	-1411	-6045	3296	0.028
2001	*-4.9*	3.1	**1458**	-1139	**319**	-5726	*2937*	**0.830**
2002	-2.9	3.6	*323*	-2051	-1728	-7454	3341	*0.000*
2003	-2.6	**6.7**	601	*-3651*	*-3050*	-10504	**>3406**	*0.000*
2004	-3.3	3.4	1022	-2874	-1852	-12356	3395	*0.000*
2005	-3.8	3.8	323	-2056	-1733	-14089	3353	*0.000*
2006	**-2.5**	4.0	640	-2025	-1385	-15474	3325	0.003
Mean	**-3.5**	**3.5**	**673**	**-1963**	**-1290**		3268	0.137
St. dev.	0.8	1.3	293	756	850		131	0.255

with T_{JJA} expressed in °C, b, b_w and P in mm, is capable to explain 75% of the variance of the simulated annual mass balance, b, as fig. 10 shows. This means that with the actual mean summer temperature of T_{JJA}=+3.5 °C at Passo della Lobbia, 1148 mm of winter snowfall, contributing to the winter mass balance, and summer precipitation in addition to the actual ones would be needed to maintain the glacier in equilibrium.

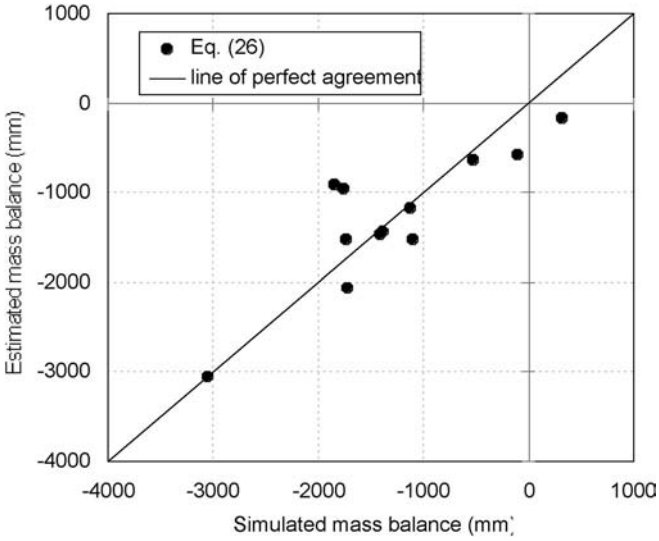

FIG. 10 - Comparison of the annual mass balance simulated by the PDSLIM model, on the x-axis, and that estimated by equation (26), on the y-axis.

Even though the mean net balance over the glacier's surface permits to evaluate the global evolution of the glacier, it does not give information about the spatial and the temporal variation of the accumulation and ablation areas; the capability of the distributed model to produce instantaneous and accumulated ablation maps, reporting the ablation rate in each cell of the glacierized area and at each time step, enables to identify local critical conditions and to project scenarios about the future evolution of the glacier, regarding the terminus position and the glacier's size and shape. Fig. 11 shows that a mean annual net balance close to –4500 mm is simulated at the glacier's terminus, and that a negative balance occurs over the whole surface with the exception of small areas over Dosson di Genova and around the Corno Bianco peak. These areas with a positive balance account for only 2% of the glacier's surface and are definetly insufficient to balance, through the glacier's flow, the dramatic losses in the ablation areas. The mean specific mass balance distribution versus altitude is shown in fig. 12 together with the glacier's hypsometry. Also the Equilibrium Line Altitude and the Accumulation Area Ratio, computed, respectively, as the mean altitude of the pixels with annual mass balance equal to ± 20 mm and the ratio of the area of positive balance to the to-

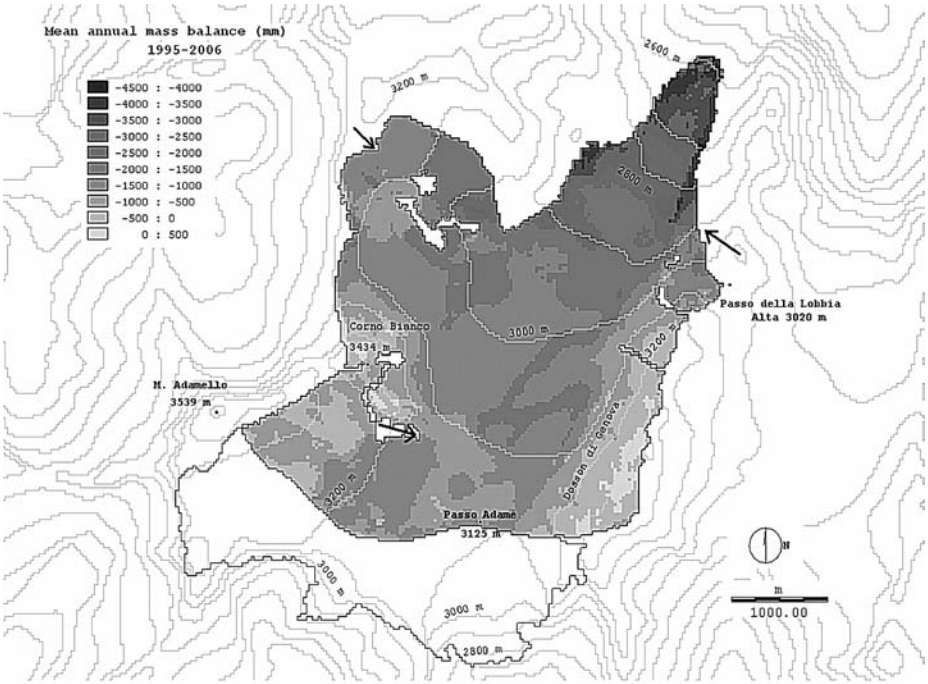

FIG. 11 - Simulated map of the mean annual mass balance of the Mandrone Glacier averaged over the twelve years period 1995-2006. Arrows indicate the direction of potential avalanches.

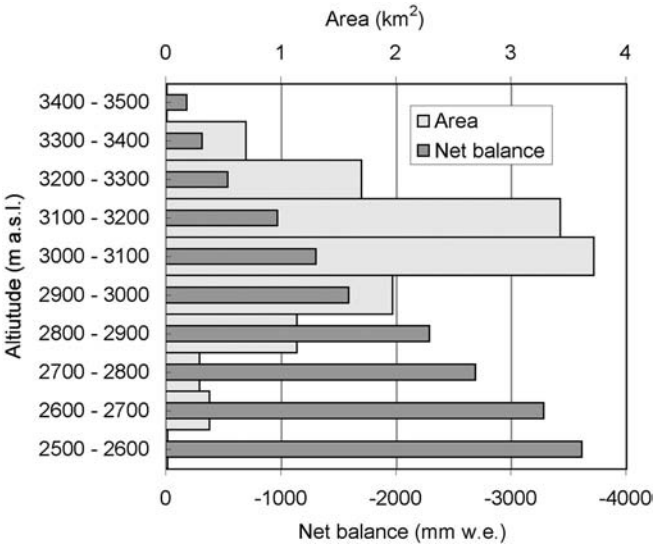

FIG. 12 - Mean 1995-2006 specific mass balance distribution versus altitude (mm w.e.) and Mandrone Glacier hypsometry.

tal glacier's area at the end of September, are reported in the last two columns of tab. 3. They confirm the negative mass balance losses computed by the model.

DISCUSSION

VERIFICATION WITH SATELLITE IMAGES AND RUNOFF DATA

ASTER images were used not only for the estimation of the ice albedo, as mentioned before, but for two further purposes. The first one was to evaluate the position of the glacier's terminus and show the progressive retreat of the glacier since 1864 (fig. 13); in this case satellite images show a retreat of about 40 m from 2002 to 2003, much more rapid compared to the previous period when it was of the order of 7.5 m a^{-1} in the 1987-2002 period, and even slower, 4 m a^{-1}, from 1953 to 2002, as documented by the

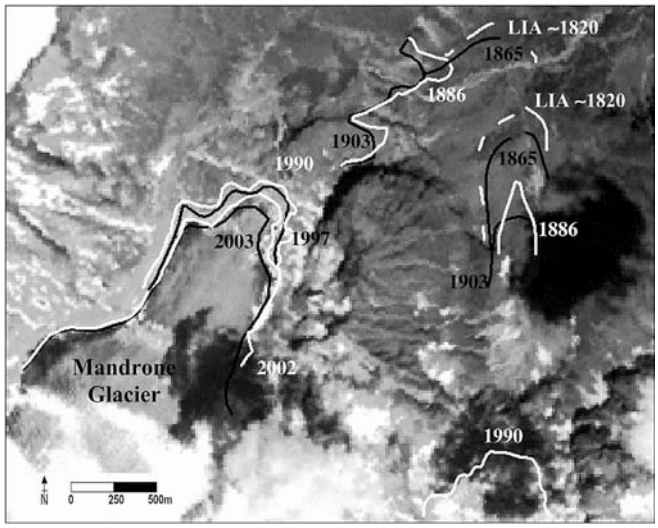

FIG. 13 - The retreat of the Mandrone glacier's terminus since the end of the Little Ice Age (dashed line drawn after Baroni and Carton, 1990) until year 2003. The position of the glacier's front is superimposed over the 20 June 2003 ASTER image and was redrawn after the analysis of five maps (Payer, 1865; K.U.K. M.I., 1886; D.Ö.A.V. 1903; Provincia Autonoma di Trento-CTR, 1990; Comitato Glaciologico Trentino web site, 1997) and of two Aster images scanned in 2002 and 2003.

terminus measurements by Marchetti (1978-1993) and Marchetti (1999-2004) collected and summarised in the WGI data base. The accumulated retreat since the Little Ice Age, as marked by the geomorphological signatures drawn on the map by Baroni & Carton (1996), is now about 2.1 km in length, corresponding to an increase of the glacier's terminus altitude of about 900 m.

Another objective was to verify the accuracy of the model in simulating the retreat of snow covered areas during the simulation period. The seasonal snowline position detected by setting a threshold on the map obtained from the radiance at sensor in the ASTER first visible band in the June 20th 2003 satellite image in fig. 14 is compared with the boundary of snow simulated by the model initialised on April 1st 2003 and run with meteorological forcing only. The pixels classified as snow-covered in both the satellite and model-simulated maps are 35256 out of 41231 pixels of the "true" snow cover as detected on the satellite map, for the Sarca di Genova at Ponte Maria basin, thus resulting in a 86% correspondence. The same verification was done for the 23rd August 2003 image: both the simulation and the satellite image showed no remaining snow-covered pixels at the end of that exceptionally hot summer.

The comparison of the satellite image scanned on June 20th 2003 and the snow depth map simulated for the same day provide a first check on the overall reliability of the snow and ice melt model setup. In fact the snowline seems to have quite the same shape and location in the two images, as shown by some key geomorphological features indicated by the black arrows. The result is however dependent upon a correct estimate of: 1) the snow water equivalent depth at the beginning of the ablation season, 2) the snowfall accumulated in the simulation period and 3) the heat fluxes estimated to compute the snow and ice melt.

A wrong estimate of any of these three variables would unavoidably introduce errors in the energy balance on the simulation domain which includes the whole Sarca di Genova basin gauged at the Vasca di Genova outlet. Wrong initial conditions, snow precipitation and simulated heat fluxes would result in a wrong location of the transient snowline compared to the observed ones.

A further comparison was done with runoff measured in the ablation season (from April to September) in the Ponte Maria streamauge shown in fig. 15. By excluding the year 2001 with an anomalous winter balance, the linear correlation coefficient between the simulated snow and ice melt and measured runoff is 0.83, thus providing a further support to the reliability of our simulations. Including the year 2001 the correlation decreases to 0.36.

Uncertainties and Future Developments

Several uncertainties can affect our results and conclusions. Although we dedicated a lot of effort to the data collection and analysis and to the reference to literature data, we are aware of the complexity of the modelling approach described here.

One of the uncertainties we consider of major relevance is related to precipitation and snow water equivalent measurements. The maintainance of reliable precipitation gauges at a high altitude is of paramount importance, as well as the correction of precipitation measurements with the altitudinal trend. The applied precipitation correction, described in the previous paragraph, increased summer

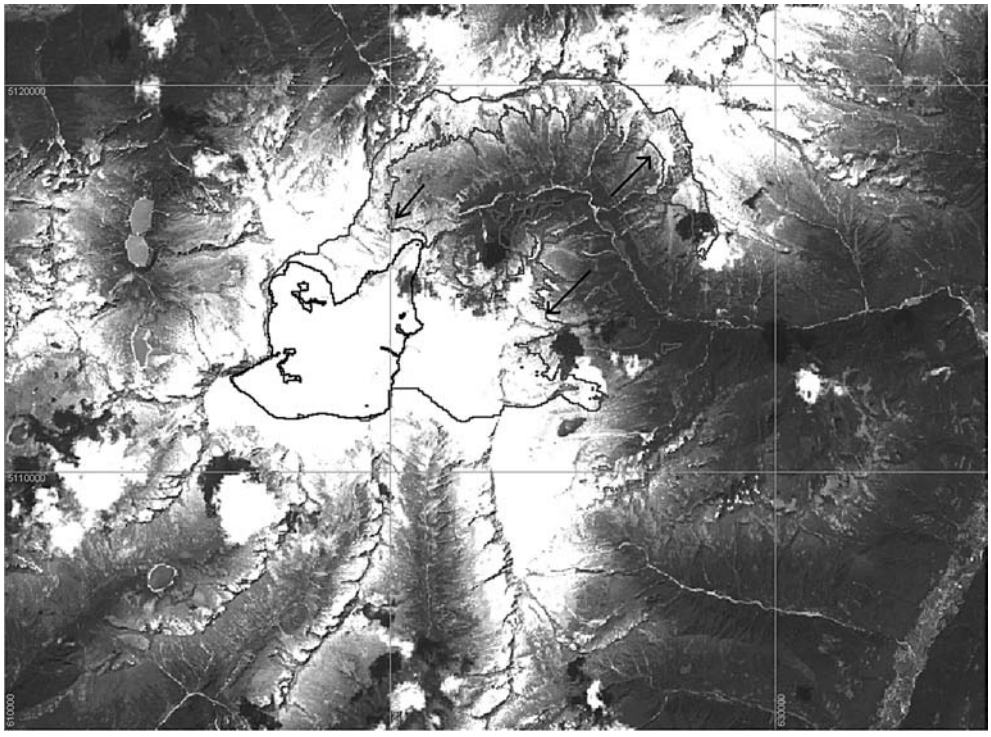

Fig. 14 - Limits of the snow line simulated by the PDSLIM model on the 20th of June 2003 (in grey) superimposed on the VNIR 1 band of the corresponding ASTER image. In black the limits of the Mandrone Glacier on the UTM coordinates grid.

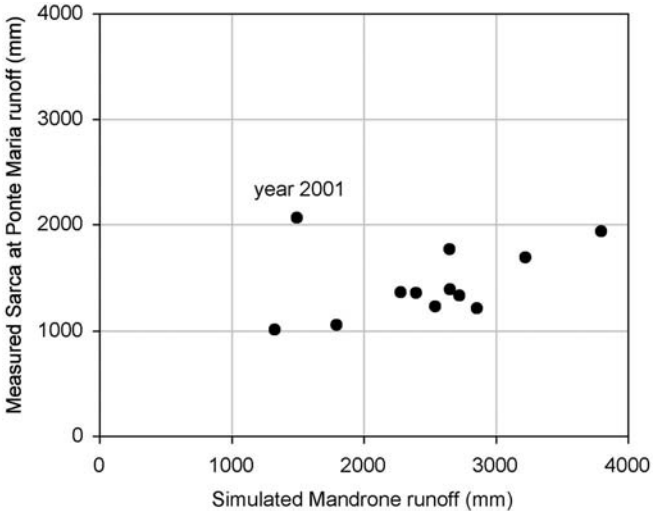

FIG. 15 - Comparison of the runoff volume measured from April to September at the Sarca di Genova at Ponte Maria station and the simulated snow and ice runoff of the Mandrone Glacier.

precipitation by 140 mm to the measured values. In addition, higher snowfall in summer has a positive feedback on the mass balance, by reducing ablation. No major improvements can be expected in the short term for snow water equivalent monitoring technologies, since point measurements in a dense network of snow gauges, such as those conducted so far, are still the backbone for snow water equivalent monitoring systems in areas as that investigated here (see, for instance, Bocchiola & Rosso, 2007). A denser network of snow gauges can, however, increase the accuracy of winter mass balance estimates. Avalanches can provide additional mass to the glacier, although their influence is limited to small areas indicated by the arrows in fig. 11.

Snow and ice aerodynamic roughness estimates and modelling of turbulent fluxes, performed by applying standard literature methods, are another source of uncertainty subject to future developments. Further verifications based on a comparison of simulated runoff with hourly discharge measurements at the Ponte Maria station, point measurements at ablation stakes conducted in 2007 and 2008 and turbulent fluxes measurements at an eddy-correlation station installed on the glacier in the summer of 2008 are now being processed, in order to reduce uncertainties of our model's results.

Despite these factors of uncertainty, we are quite confident about the reliability of our conclusions, based on our point and distributed measurements, runoff data and the fairly good agreement between our mass balances and those obtained with the glaciological method in the nearby, south-east facing Caresèr Glacier (Zanon, 1992; Carturan & Seppi, 2007). The comparison of the accumulated mass balance modelled with the energy-balance method for the Mandrone Glacier with that measured on the Caresèr Glacier was shown in fig. 9 which illustrates a qualitative and quantitative agreement between the two time series. A more negative balance for the Caresèr Glacier is justified by its lower altitude, ranging from 2860 m and 3310 m a.s.l. and its south-east facing orientation. The most negative and positive balance years, and also the time series of the Equilibrium Line Altitude and Accumulation Area Ratio of the two glaciers, exhibit a similar time pattern as shown by the comparison of our data in tab. 3 with those reported by Carturan & Seppi (2007), with a maximum of the AAR in the year 2000/01 and a maximum of the ELA in the year 2002/03 for both glaciers. This means that, according to our simulation framework, if the meteorological conditions observed over the 1995-2006 period are representative of the future climate, it is very reasonable to expect that the equilibrium shape and size of the glacier will be much different and smaller than the actual ones. Assuming an accumulation area ratio close to 0.5 in equilibrium conditions, it can be projected that only small glacierised areas over Dosson di Genova and around Corno Bianco above 3200 m a.s.l. might survive in the future. Climate warming, as that projected for this area by several Global Circulation Models (see Barontini & *alii*, 2009) would further reduce the glacier's areas and possibly lead to a complete disappearance of the Mandrone glacier.

CONCLUSIONS

The mass balance of the Mandrone Glacier, which is the major hydrographic unit of the largest glacierised area of the southern Alps, has been evaluated for twelve years, from 1995 up to 2006. The evaluation was performed by applying the PDSLIM distributed energy balance model, already tested both at the point and at the basin scale in different alpine basins. For the model's setup albedo maps derived from satellite imagery were adopted, with point measurements used for verification. Even if some precipitation gauges are located at high elevation within the basin, a corrrection factor for the precipitation value had to be adopted in order to take into account the observed orographic enhancement of precipitation, a frequent phenomenon in mountain areas. A precipitation lapse rate was then used to correct 651 mm of observed April to September precipitation to 791 mm of corrected precipitation.

A mean value of the annual mass balance of –1290 mm results, with a high inter-annual variability, which can be well explained in terms of summer temperature and summer precipitation added to winter mass balance. Only 2% of the glacier's area has a positive mass balance.

For verification, 86% of the satellite-derived transient snow-covered area was in agreement with that simulated by the model eighty days after the model's initialisation. A new discharge rating curve for the Sarca di Genova at Ponte Maria was calibrated on the basis of seven measurements. The resulting summer runoff measurement is highly correlated with the simulated snow and ice-melt over the Mandrone Glacier.

The major uncertainties affecting this type of method to compute the glacier's mass balance lay in the precipita-

tion measurements at high altitude and in the definition of the initial state of the basin in April. In particular the snow water equivalent can be affected by avalanches in some small areas and in the parameterisation of turbulent fluxes. Developments which are currently in progress include the verification of ablation with a network of ablation stakes, the analysis of eddy-correlation measurements conducted in 2008 and hourly runoff simulated at the Ponte Maria streamgauge.

With the high negative balance and the climate of the recent years the actual geomorphological condition of the Mandrone Glacier is far from an equilibrium and a significant shrinkage and volume loss of the glacier is expected for the near future. The methodology used for this analysis can be applied considering future climatic scenarios which would likely result in even more negative mass balances.

In perspective, this study can be useful also to assess changes on the runoff and sediment transport regime, as well as on the impact on downstream hydropower generation capacity and water resources available for irrigation and environment conservation.

REFERENCES

AUER I., BÖHM R., JURKOVIC A., LIPA W., ORLIK A., POTZMANN R., SCHOENER W., UNGERSBOECK M., MATULLA C., BRIFFA K., JONES P., EFTHYMIADIS D., BRUNETTI M., NANNI T., MAUGERI M., MERCALLI L., MESTRE O., MOISSELIN J.-M., BEGERT M., MUELLER-WESTERMEIER G., KVETON V., BOCHNICEK O., STASTNY P., LAPIN M., SZALAI S., SZENTIMREY T., CEGNAR T., DOLINAR M., GAJIC-CAPKA M., ZANINOVIC K., MAJSTOROVIC Z., & NIEPLOVA E. (2007) - *HISTALP - historical instrumental climatological surface time series of the Greater Alpine Region*, International Journal of Climatology, 27, 17-46.

ASTORI B. & TOGLIATTI G. (1964) - *Il rilievo aerofotogrammetrico del ghiacciaio Pian di Neve (Adamello).* Bollettino del Comitato Glaciologico Italiano, serie 2, 11 (1), 33-50.

BARONI C. & CARTON A. (1990) - *Variazioni oloceniche della Vedretta della Lobbia (Gruppo dell'Adamello Alpi Centrali).* Geografia Fisica e Dinamica Quaternaria, 13, 105-119.

BARONI C. & CARTON A. (1996) - *Geomorfologia dell'alta Val di Genova (Gruppo dell'Adamello Alpi Centrali).* Geografia Fisica e Dinamica Quaternaria, 19, 3-17.

BARONI C., CARTON A., MARTINELLI N. & PIGNATELLI O. (1992) - *Dendrocronologia e variazioni glaciali oloceniche in Val di Genova (M. Adamello, Alpi Centrali). Nota preliminare.* Geografia Fisica e Dinamica Quaternaria, 15, 30-40.

BARONI C., CARTON A. & SEPPI R. (2004) - *Distribution and behaviour of rock glaciers in the Adamello-Presanella Massif (Italian Alps).* Permafrost and Periglacial Processes, 15 (3), 243-259.

BARONTINI S., GROSSI G., KOUWEN N., MARAN S., SCARONI P. & RANZI R. (2009) - *Impacts of climate change scenarios on runoff regimes in the southern Alps*, Hydrology and Earth System Sciences Discussions, 6, 3089-3141.

BENISTON M. (1997) *Variations of snow depth and duration in the Swiss Alps over the last 50 years: links to changes in large-scale climatic forcings*. Climate Change, 36, 281-300.

BOCCHIOLA D. & ROSSO R. (2007) - *The distribution of daily snow water equivalent in the central Italian Alps*, Advances in Water Resources, 30, 135-147.

BROCK B.W., WILLIS I.C. & SHARP M.J. (2006) - *Measurements and parametrization of aerodynamic roughness length variation at Haut Glacier d'Arolla, Switzerland.* Journal of Glaciology, 52 (177), 281-297.

BRUNETTI M., MAUGERI M. & NANNI T. (2000) *Variations of temperature and precipitation in Italy from 1866 to 1995*. Advances in Water Resources, 65, 165-174.

CAGNATI A., CREPAZ A., MACELLONI G., PAMPALONI P., RANZI R., TEDESCO M., TOMIROTTI M. & VALT M. (2004) - *Study of the snow melt-freeze cycle using multi-sensor data and snow modelling.* Journal of Glaciology, 50 (170), 419-426.

CARABELLI E. (1961) - *Misure sismiche di spessore del ghiacciaio Pian di Neve (Adamello).* Bollettino del Comitato Glaciologico Italiano, serie 2, 11 (1), 51-60.

CALMANTI S., MOTTA L., TURCO M. & PROVENZALE A. (2007) - *Impact of climate variability on Alpine glaciers in northwestern Italy*, International Journal of Climatology, 27, 2041-2053.

CARTURAN L. & SEPPI R.(2007) - *Recent mass balance results and morphological evolution of Careser Glaciers (Central Alps).* Geografia Fisica e Dinamica Quaternaria, 30 (1), 33-42.

CITTERIO M., DIOLAIUTI G., SMIRAGLIA C., D'AGATA C., CARNIELLI T., STELLA G. & SILETTO G.B. (2007) - *The fluctuations of Italian glaciers during the last century: a contribution to knowledge about Alpine glacier changes*. Geografiska Annaler, 89, A3, 164-182.

COMITATO GLACIOLOGICO ITALIANO - C.N.R. (1961) - *Catasto dei ghiacciai italiani. Anno geofisico 1957-1958. III: Ghiacciai della Lombardia e dell'Ortles-Cevedale,* Torino, 389 pp.

C.G.T. - COMITATO GLACIOLOGICO TRENTINO (1994) - *I ghiacciai del Parco Naturale Adamello-Brenta. Catasto a cura del Comitato Glaciologico del Trentino*, Parco Adamello Brenta, Nuova Stampa Rapida, Trento, 126 pp.

DENBY B. & GREUELL W. (2000) - *The use of bulk and profile methods for determining surface heat fluxes in the presence of glacier winds.* Journal of Glaciology, 46 (154), 445-452.

DIOLAIUTI G., SMIRAGLIA C., REYNAUD L., D'AGATA C. & PAVAN M. (2002) - *Relation entre les bilans de masse de la Sforzellina et ceux des autres glaciers en Europe. Influence des facteurs localisation géographique et taille du glacier.* La Houille Blanche. vol. 6/7, 1-5.

D.Ö.A.V. - DEUTSCHER UND ÖSTERREICHISCHER ALPENVEREIN (1903) - *Karte der Adamello und Presanella Gruppe. Scale 1:50000,* Zeitschrift der DÖAV.

FRASSONI A., ROSSI G.C. & TAMBURINI A. (2001) - *Studio del ghiacciaio dell'Adamello mediante indagini georadar.* Supplemento di Geografia Fisica e Dinamica Quaternaria, V, 77-84.

GIADA M. & ZANON G. (1996) - *Elevation and volume changes in the Careser glacier (Ortles-Cevedale group, Central Alps)*, Zeitschrift für Gletscherkunde und Glazialgeologie, 31, 143-147.

GROSSI G. & FALAPPI L. (2003) - *Comparison of energy fluxes at the land surface-atmosphere interface in an Alpine valley as simulated with different models*, Hydrology and Earth System Sciences, 7 (6), 920-936.

HOCK R. (1998) - *Glacier Melt and discharge: a review of processes and their modelling. In Modelling of Glacier Melt and Discharge,* Zurcher Geographische Schriften, Heft 70, Geographisches Institut ETH, Zurich.

HOCK R. & HOLMGREN B. (2005) - *A distributed surface energy-balance model for complex topography and its application to Störglaciaren, Sweden.* Journal of Glaciology, 51 (172), 25-36.

IPCC (2007) - *Climate Change 2007: Synthesis Report. Contribution of Working Groups I, II and III to the Fourth Assessment Report of the Intergovernmental Panel on Climate Change.* Core Writing Team, Pachauri R.K & Reisinger A. (eds.), IPCC, Geneva, Switzerland.

KARGEL J.S., ABRAMS M.J., BISHOP M.P., BUSH A., HAMILTON G., JISKOOT H., KÄÄB A., KIEFFER H.H., LEE E.M., PAUL F., RAU F., RAUP B., SHRODER J.F., SOLTESZ D., STEARNS L., WESSELS R. & THE GLIMS CONSORTIUM (2005) - *Multispectral imaging contributions to Global Land Ice Measurements from Space*. Remote Sensing of Environment, 99, 187-219.

KASER G., MUNARI M., NOGGLER B., OBERSHIEMD C. & VALENTINI P. (1995) - *Ricerche sul bilancio di massa del ghiacciaio di Fontana Bianca (Weissbrunnferner) nel gruppo Ortles-Cevedale,* Geografia Fisica e Dinamica Quaternaria, 18, 277-280.

KASER G., FOUNTAIN A. & JANSSON P. (2003) - *A manual for monitoring the mass balance of mountain glaciers*, IHP Technical Documents in Hydrology No. 59, UNESCO, Paris, 107 pp.

KLOK E.J. & OERLEMANS J. (2002) - *Model study of the spatial distribution of the energy and mass balance of Morteratschgletscher, Switzerland*, Journal of Glaciology 48 (163), 505-518.

K.U.K.M.I. - KEISERLICH UND KÖNIGLICH MILITÄRGEOGRAPHISCHES INSTITUT (1886) - *Karte Tione und M. Adamello - Scale 1:75000.*

KUHN M. (1979) - *Climate and glaciers.* In: I. Allison (ed.) «Sea Level, Ice, and Climate Change», IAHS Publications, 131, 3-20.

KUHN M., MARKL G., KASER G., NICKUS U., OBLEITNER F. & SCHNEIDER H. (1985) - *Fluctuations of climate and mass balance: different responses of two adjacent glaciers.* Zeitschrift für Gletscherkunde und Glazialgeologie, 21, 409-416.

LATERNSER M. & SCHNEEBELI M. (2003) - *Long-term snow climate trends of the Swiss Alps (1931-99)*, International Journal of Climatology, 23, 733-750.

MACELLONI G., PALOSCIA S., PAMPALONI P., BROGIONI M., RANZI R. & CREPAZ A. (2005) - *Monitoring of melting refreezing cycles of snow with microwave radiometers: The Microwave Alpine Snow Melting Experiment* (MASMEx 2002-2003). IEEE Transactions on Geoscience and Remote Sensing, 43 (11), 2431-2441.

MARAGNO D., DIOLAIUTI G., D'AGATA C., MIHALCEA C., BOCCHIOLA D., BIANCHI JANETTI E., RICCARDI A. & SMIRAGLIA C. (2009) - *New evidence from Italy (Adamello Group, Lombardy) for analysing the ongoing decline of Alpine glaciers*, Geografia Fisica e Dinamica Quaternaria, 32, 31-39.

MARCHETTI V. (1978-1993) - *Relazioni delle campagne glaciologiche: Gruppo Adamello-Presanella (versante trentino). Ghiacciai della Lobbia e del Mandron.* Geografia Fisica e Dinamica Quaternaria, 1(1) (1978); 2 (2) (1979); 3 (2) (1980); 4 (2) (1981); 5 (2) (1982); 7 (2) (1985); 9 (1) (1987); 9 (1) (1987); 10 (2) (1988); 11 (2) (1989); 12 (2) (1990); 13 (2) (1991); 14 (2) (1992); 15 (1993).

MARCHETTI F. (1999-2004) - *Relazioni delle campagne glaciologiche: Ghiacciai del Gruppo Adamello-Presanella. Ghiacciaio del Mandron.* Geografia Fisica e Dinamica Quaternaria, 22 (2) (1999); 23 (2) (2000); 24 (2) (2001); 25 (2) (2002); 26 (2) (2003); 27 (2) (2004).

OHMURA A., KASSER P. & FUNK M. (1992) - *Climate at the equilibrium line of glaciers*, Journal of Glaciology, 38 (130), 397-411.

PATERSON W.S.B. (1994) - *The physics of glaciers,* Pergamon Press.

PAUL F., KÄÄB A., MAISCH M., KELLENBERGER T. & HAEBERLI W. (2004) - *Rapid disintegration of alpine glaciers observed with satellite data*. Geophysical Research Letters, 31, L21402.

PAYER J. (1865) - *Die Adamello-Presanella-Alpen nach den Forschungen und Aufnahmen von Julius Payer* - Scala 1:56000, Petermann's Geographischen Mitteilungen, ed. Justus Perthes, Gotha, 11 (17), 36 pp.

PLÜSS C. & MAZZONI R. (1994) - *The role of turbulent heat fluxes in the energy balance of high alpine snow cover.* Nordic Hydrology, 25, 25-38.

RANZI R. & ROSSO R. (1991) - *A physically based approach to modelling distributed snowmelt in a small alpine catchment.* In: Bergmann H., Lang H., Frey W., Issler D. & Salm B. (eds.), «Snow Hydrology and Forests in High Alpine Areas», IAHS Publications, 205, 141-150.

RANZI R. & ROSSO R. (1995) - *Distributed estimation of incoming direct solar radiation over a drainage basin*. Journal of Hydrology, 166 (3-4), 461-478.

RANZI R., GROSSI G. & BACCHI B. (1999) - *Ten years of monitoring areal snowpack in the Southern Alps using NOAA-AVHRR imagery, ground measurements and hydrological data*. Hydrological Processes, 13 (12-13), 2079-2095.

RANZI R., GROSSI G., IACOVELLI L. & TASCHNER S. (2004) - *Use of multispectral ASTER images for mapping debris-covered glaciers within the GLIMS project.* International Geoscience and Remote Sensing Symposium (IGARSS), 2, 1144-1147.

RANZI R. & TASCHNER S. (2005) - *Energy and hydrological balance of the Adamello Glacier as an indication of current climate change*, Geophysical Research Abstracts, 7, 06404.

SANTILLI M., OROMBELLI G. & PELFINI M. (2002) - *Variations of Italian glaciers between 1980 and 1999 inferred by the data supplied by the Italian Glaciological Committee.* Geografia Fisica e Dinamica Quaternaria, 25, 61-76.

S.G.L. - SERVIZIO GLACIOLOGICO LOMBARDO (1992) - *Ghiacciai in Lombardia*, Edizioni Bolis, Bergamo, Italy.

SMEETS C.J.P.P., DUYNKERKE P.G., VUGTS H.F., *Turbulence characteristics of the stable boundary layer over a mid-latitude glacier. Part I: a combination of katabatic and large-scale forcing*, Boundary-Layer Meteorology, 87, 117-145, 1998.

SMEETS C.J.P.P., DUYNKERKE P.G. & VUGTS H.F., *Turbulence characteristics of the stable boundary layer over a mid-latitude glacier. Part II: pure katabatic forcing conditions*, Boundary-Layer Meteorology, 97, 73-107, 2000.

WGMS (2008) - *Global Glaciers changes: facts and figures*, Zemp M., Roer I, Kääb A., Hoelzle M., Paul F., and Haeberli W. (eds), UNEP, World Glacier Monitoring Service, Zurich, Switzerland, 88 pp.

ZANON G. (1992) - *Venticinque anni di bilancio di massa del ghiacciaio del Careser, 1966-67/1990-91.* Geografia Fisica e Dinamica Quaternaria, 15, 215-220.

(Ms. presented 10 October 2009; accepted 1 April 2010)